Desalination and Water Treatment
www.deswater.com

doi: 10.1080/19443994.2015.1082944

57 (2016) 16288–16299
July

Taylor & Francis
Taylor & Francis Group

Evaporation of water/ammonia binary liquid film falling down on one plate of a vertical channel

Abdelaziz Nasr[a,b,*], Abdulmajeed S. Al-Ghamdi[b,*]

[a]*Laboratory of Thermal and Energy Systems Studies, Monastir University, Ibn Eljazzar Street, 5019 Monastir, Tunisia, Tel. +966 1252 700 70; Fax: +966 1252 700 27; emails: abdelaziz.nasr@ymail.com (A. Nasr), asaalghamdi@uqu.edu.sa (A.S. Al-Ghamdi)*
[b]*Mechanical Engineering Department, College of Engineering, Umm Al-Qura University, Makkah P.O. Box 5555, Kingdom of Saudi Arabia*

Received 16 February 2015; Accepted 3 August 2015

ABSTRACT

A numerical study was conducted to investigate the coupled heat and mass transfer during the evaporation of a water/ammonia liquid film under mixed convection. This binary liquid film is falling down on one plate of a vertical channel. The wetted plate is adiabatic while the dry plate is isothermal. Parametric computations were performed to investigate the effects of the inlet parameters of the water/ammonia binary liquid film on the temperature at the liquid–gas interface and on the mixture evaporation rate.

Keywords: Water/ammonia film; Evaporation; Heat and mass transfer; Mixed convection; Binary liquid film

1. Introduction

Falling film evaporation is found in many industrial applications such as chemical engineering, combustion premixing, refrigeration technology, desalination, separation processes, cooling towers, air conditioning and heat transformers.

Hoke and Chen [1] numerically investigated the binary liquid film evaporation on a vertical plate. They analysed the evolution of two dimensionless numbers (Nusselt and Sherwood). Wang [2] presented the evaporation of the ternary liquid film. The simultaneous mass and heat transfer in evaporating multicomponent films was presented and investigated. Armouzi et al. [3] numerically analysed the evaporation of a binary liquid film flowing inside a cylindrical channel. They analysed the effect of the volatilities of the liquid film on the evaporation and on the coupled mass and heat transfer. Palen et al. [4] experimentally treated the evaporation of an ethylene glycol–water mixture liquid film. An approximate film-theory formulation was used with the mass-transfer coefficients for the falling films found from the experimental data. The correlations in terms of Sherwood, Schmidt and Reynolds numbers were presented. A numerical study of the combined mass and heat transfer in evaporation of a two-component liquid film flow was performed by Baumann and Thiele [5]. The influence of the phase equilibrium on the benzene-methanol evaporation was analysed. O'Hare and Spedding [6] experimentally studied the evaporation of the water–ethanol binary liquid mixture on a horizontal plate. The effect of the composition of binary liquid mixture on the total evaporating rate was studied. Ziobrowski et al. [7] theoretically and experimentally studied the evaporation of water/isopropanol binary

*Corresponding authors.

liquid film. The numerical and experimental data of evaporation of water–isopropanol binary liquid film were compared. Cherif and Daif [8] conducted a numerical study of the evaporation of binary liquid film flowing of one of the two parallel plates. The influence of the inlet liquid composition on the heat and mass transfers was analysed. Results revealed that the film thickness cannot be neglected for the second mixture (ethylene glycol–water). Agunaoun et al. [9] numerically investigated the binary liquid film evaporation on an inclined plate. Results indicated that it is possible to evaporate more water when the inlet liquid mass fraction of ethylene glycol is less than 40%. Nasr et al. [10] reported a numerical analysis of binary liquid film evaporation on a vertical plate. Results showed that, it is possible to increase the water and the mixture evaporation, when the inlet liquid concentration of ethylene glycol is less than a particular value. Hfaiedh et al. [11] numerically treated the water–ethylene-glycol film evaporation on a vertical channel. Results indicated that from an inversion distance and from a liquid inversion concentration of ethylene glycol, it is possible to evaporate more water than if the film at the entry was pure water only.

This literature review shows that the problem of the numerical study of evaporation of water/ammonia mixture liquid film falling on vertical plate has not been sufficiently studied. The purpose of this paper is to discuss the effects of the inlet parameters of the binary film on the temperature at the liquid–gas interface and on the total cumulated evaporation rate of liquid mixture.

2. Analysis

This paper presents the results of a numerical analysis of the evaporation under mixed convection of a binary liquid film falling along a vertical channel (Fig. 1(a)). The studied channel is consisting of two parallel plates. The first plate is adiabatic and wetted by a binary liquid film (water–ammonia), while the second one is dry and isothermal. The falling mixture liquid enters the first plate with an inlet temperature T_{0L}, inlet mass flow rate m_{L0} and inlet liquid composition of ammonia $c_{liq,ethylene\ glycol}$. The air enters the channel with a temperature T_0, water and ammonia vapour concentrations c_{01} and c_{02} and velocity u_0.

2.1. Governing equations

The equations governing the flow and coupled mass and heat transfers in the liquid and in the gas phases (Appendix 1) are as follows [8,9].

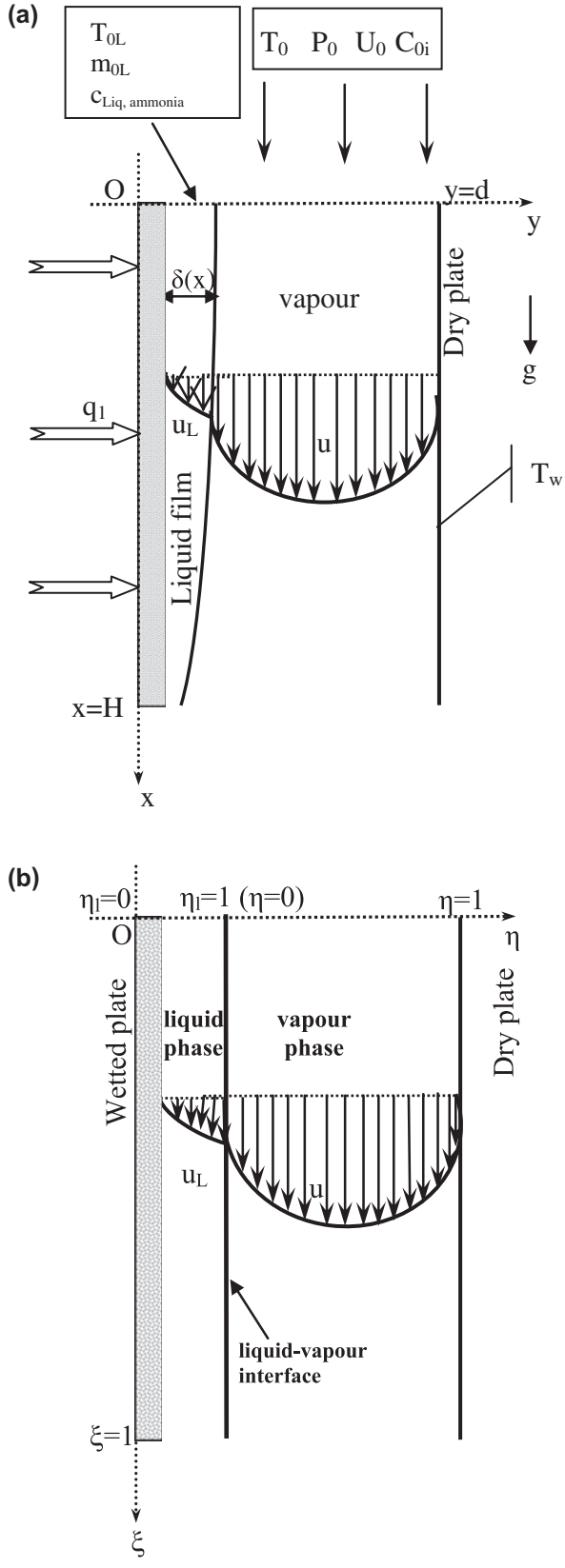

Fig. 1. Physical model.

(1) For the liquid phase

The liquid mixture consists of two components (water + ammonia).

Continuity equation

$$\frac{\partial \rho_L u_L}{\partial \xi} - \frac{\eta_L}{\delta}\frac{\partial \delta}{\partial \xi}\frac{\partial \rho_L u_L}{\partial \eta_L} + \frac{H}{\delta}\frac{\partial \rho_L v_L}{\partial \eta_L} = 0 \tag{1}$$

x-momentum equation

$$u_L\frac{\partial u_L}{\partial \xi} + \left(v_L\frac{H}{\delta} - u_L\frac{\eta_L}{\delta}\frac{\partial \delta}{\partial \xi}\right)\frac{\partial u_L}{\partial \eta_L} = -\frac{1}{\rho_L}\frac{dP}{d\xi} - \frac{H}{\rho_L \delta^2}\frac{\partial}{\partial \eta_L}\left[\mu_L\frac{\partial u_L}{\partial \eta_L}\right] + gH \tag{2}$$

Energy equation

$$u_L\frac{\partial T_L}{\partial \xi} + \left(u_L\frac{\eta_L - 1}{\delta}\frac{\partial \delta}{\partial \xi} + \frac{H}{\delta}v_L\right)\frac{\partial T_L}{\partial \eta_L} = \frac{1}{\rho_L C_{pL}}\left\{\frac{H}{\delta^2}\frac{\partial}{\partial \eta_L}\left(\lambda_L\frac{\partial T_L}{\partial \eta_L}\right) + \rho_L D_L(C_{pL,1} - C_{pL,2})\frac{H}{\delta^2}\frac{\partial T_L}{\partial \eta_L}\frac{\partial C_{L,1}}{\partial \eta_L}\right\} \tag{3}$$

where D_L is the mass diffusivity of species i.

Species diffusion equations

$$u_L\frac{\partial c_{Li}}{\partial \xi} + \left(u_L\frac{\eta_L - 1}{\delta}\frac{\partial \delta}{\partial \xi} + \frac{H}{\delta}v_L\right)\frac{\partial c_{Li}}{\partial \eta_L} = \frac{1}{\rho_L}\frac{H}{\delta^2}\frac{\partial}{\partial \eta_L}\left(\rho_L D_L\frac{\partial c_{Li}}{\partial \eta_L}\right); \quad i = 1,\ 2 \tag{4}$$

where $c_{L1} + c_{L2} = 1$.

The overall mass balance equation

$$\int_0^1 \delta \rho_L u_L d\eta_L = \left[m_{0L} - H\int_0^\xi \rho V(\xi,\ \eta = 0)d\xi\right] \tag{5}$$

(2) For the gaseous phase

The gas mixture consists of water vapour, ammonia vapour and dry air.

Continuity equation

$$\frac{\partial \rho u}{\partial \xi} + \frac{\eta - 1}{d - \delta}\frac{\partial \delta}{\partial \xi}\frac{\partial \rho u}{\partial \eta} + \frac{H}{d - \delta}\frac{\partial \rho v}{\partial \eta} = 0 \tag{6}$$

x-momentum equation

$$u\frac{\partial u}{\partial \xi} + \left(\frac{\eta - 1}{d - \delta}\frac{\partial \delta}{\partial \xi}u + \frac{H}{d - \delta}v\right)\frac{\partial u}{\partial \eta} = -\frac{1}{\rho}\frac{dP}{d\xi} - g\beta H(T - T_0) - g\beta^* H\sum_{i=1}^{2}(c_i - c_{0i}) + \frac{1}{\rho}\frac{H}{(d - \delta)^2}\frac{\partial}{\partial \eta}\left(\mu\frac{\partial u}{\partial \eta}\right) \tag{7}$$

Energy equation

$$u\frac{\partial T}{\partial \xi} + \left(u\frac{\eta - 1}{d - \delta}\frac{\partial \delta}{\partial \xi} + \frac{H}{d - \delta}v\right)\frac{\partial T}{\partial \eta} = \frac{1}{\rho C_p}\left\{\frac{H}{(d - \delta)^2}\frac{\partial}{\partial \eta}\left(\lambda\frac{\partial T}{\partial \eta}\right) + \rho\sum_{i=1}^{2}(D_{g,im}c_{pi} - D_{g,am}c_{pa})\frac{H}{(d - \delta)^2}\frac{\partial T}{\partial \eta}\frac{\partial c_i}{\partial \eta}\right\} \tag{8}$$

where $D_{g,im}$ and $D_{g,am}$ are respectively the mass diffusivity of the vapour i and of dry air given by [9,12,13].

Species diffusion equations

$$u\frac{\partial c_i}{\partial \xi} + \left(u\frac{\eta - 1}{d - \delta}\frac{\partial \delta}{\partial \xi} + \frac{H}{d - \delta}v\right)\frac{\partial c_i}{\partial \eta} = \frac{1}{\rho}\frac{H}{(d - \delta)^2}\frac{\partial}{\partial \eta}\left(\rho D_{g,im}\frac{\partial c_i}{\partial \eta}\right); \quad i = 1,\ 2,\ 3 \tag{9}$$

where $c_1 + c_2 + c_3 = 1$.

The overall mass balance equation

$$\int_0^1 \rho(d - \delta)u(\xi,\ \eta)d\eta = \left[(d - \delta_0)\rho_0 u_0 + H\int_0^\xi \rho v(\xi,\ \eta = 0)d\xi\right] \tag{10}$$

2.2. Boundary conditions

For $\xi = 0$ (inlet conditions):

$$T(0,\ \eta) = T_0;\ c_1(0,\ \eta) = c_{01};\ c_2(0,\ \eta) = c_{02};\quad u(0,\ \eta) = u_0;\ P = P_0 \tag{11}$$

$$T_L(0,\ \eta_L) = T_{0L};\ \delta(0) = \delta_0;\ \int_0^1 \rho_{0L}\delta_0 u_L(0,\ \eta_L)d\eta_L = m_{0L};\ c_{Li}(0,\ \eta_L) = c_{0Li} \tag{12}$$

At $\eta = 1$ (dry plate):

$$u(\xi,\ 1) = 0;\ v(\xi,\ 1) = 0;\ T\ (\xi,\ 1) = T_w;\quad \left.\frac{\partial c_i}{\partial \eta}\right)_{\eta=1} = 0 \tag{13}$$

At $(\eta_L = 1)$ (wet plate):

$$u_L(\xi,\ 0) = 0;\quad v_L(\xi,\ 0) = 0;\quad q_1 = -\lambda_L \frac{1}{\delta}\left.\frac{\partial T_L}{\partial \eta_L}\right)_{\eta_L=0};\quad \left.\frac{\partial c_{Li}}{\partial \eta_L}\right)_{\eta_L=0} = 0 \tag{14}$$

with c_{Li} is the mass fraction of species i in the liquid film mixture.

At $\eta = 0$ $(\eta_L = 1)$ (liquid–gas interface):

The continuities of the velocities and temperatures give:

$$u_L(\xi,\ \eta_L = 1) = u(\xi,\ \eta = 0);\quad T_L(\xi,\ \eta_L = 1) = T(\xi,\ \eta = 0) \tag{15}$$

The heat balance at the interface implies [8,9,14,15]:

$$-\frac{1}{\delta}\lambda_L\left.\frac{\partial T_L}{\partial \eta_L}\right)_{\eta_L=1} = -\frac{1}{d-\delta}\lambda\left.\frac{\partial T}{\partial \eta}\right)_{\eta=0} - \dot{m}L_v \text{ with } \dot{m} = -\frac{\rho\sum_{i=1}^{2} D_{g,im}\left.\frac{\partial c_i}{\partial \eta}\right)_{\eta=0}}{(d-\delta)\left(1-\sum_{i=1}^{2} c_i(\xi,\ \eta\ =\ 0)\right)} \tag{16}$$

where L_v is the latent heat of evaporation of liquid mixture.

the concentration of species i vapour can be evaluated by [8,9]:

$$c_1(\xi,0) = \frac{p^*_{vs1}}{p^*_{vs1} + \left[p^*_{vs2}\ \frac{M_2}{M_1}\right] + \left[p - p^*_{vs1} - p^*_{vs2}\right]\frac{M_a}{M_1}};\quad c_2(\xi,0) = \frac{p^*_{vs2}}{p^*_{vs2} + \left[p^*_{vs1}\ \frac{M_1}{M_2}\right] + \left[p - p^*_{vs1} - p^*_{vs2}\right]\frac{M_a}{M_2}} \tag{17}$$

where p^*_{vsi} is the partial pressure of species i at the gas–liquid interface given by [8,9,13]:

$p^*_{vsi} = w_{Li}p_{vsi}(T)$ $(i = 1,\ 2)$; $p_{vsi}(T)$ is the pressure of saturated vapour of species i given by [8,9,14,15]:

$$p_{vs1} = 10^{17.443-[2975/T+3.68\log(T)]}\times 10^5;\quad p_{vs2} = 6894.8\exp[16.44 - 10978.8/(9T/5 - 49)]$$

The transverse velocity component of the mixture at the interface [8]:

$$v(\xi,\ \eta = 0) = -\frac{\frac{1}{d-\delta}\sum_{i=1}^{2} D_{g,im}\left.\frac{\partial c_i}{\partial \eta}\right)_{\eta=0}}{1-\sum_{i=1}^{2} c_i(\xi,\ \eta\ =\ 0)} \tag{18}$$

The continuities of shear stress and local evaporated mass flux of species i [8,9] give:

Table 1
Comparison of total evaporating rate (10^5 Mr) (kg s^{-1} m^{-2}) for various grid arrangements for $T_0 = 20$°C; $T_{0L} = 10$°C; $m_{0L} = 0.001$ kg/m s; $T_w = 20$°C; $c_{Liq,water} = c_{Liq,ammonia} = 0.5$ (50% water–ammonia mixture); $c_{01} = 0$; $c_{02} = 0$; $q_1 = 0$; $p_0 = 9$ bars; $d/H = 0.015$; $u_0 = 0.75$ m/s

$I \times J \times K$ grid point	$x = 0.2$	$x = 0.4$	$x = 0.6$	$x = 0.8$	$x = 1$
51 × (51 + 31)	13.4607	19.8265	24.9689	30.4598	35.8932
101 × (51 + 31)	13.3546	19.7192	24.7733	30.5067	35.9063
101 × (31 + 31)	13.5511	19.9013	24.5764	30.4485	35.8801
101 × (51 + 51)	13.7518	19.8017	24.6978	30.6153	35.8519
151 × (51 + 51)	13.1332	19.6986	24.9041	30.5396	35.9105

Notes: I: total grid points in the axial direction; J: total grid points in the transverse direction in the gaseous phase; K: total grid points in the transverse direction in the liquid phase.

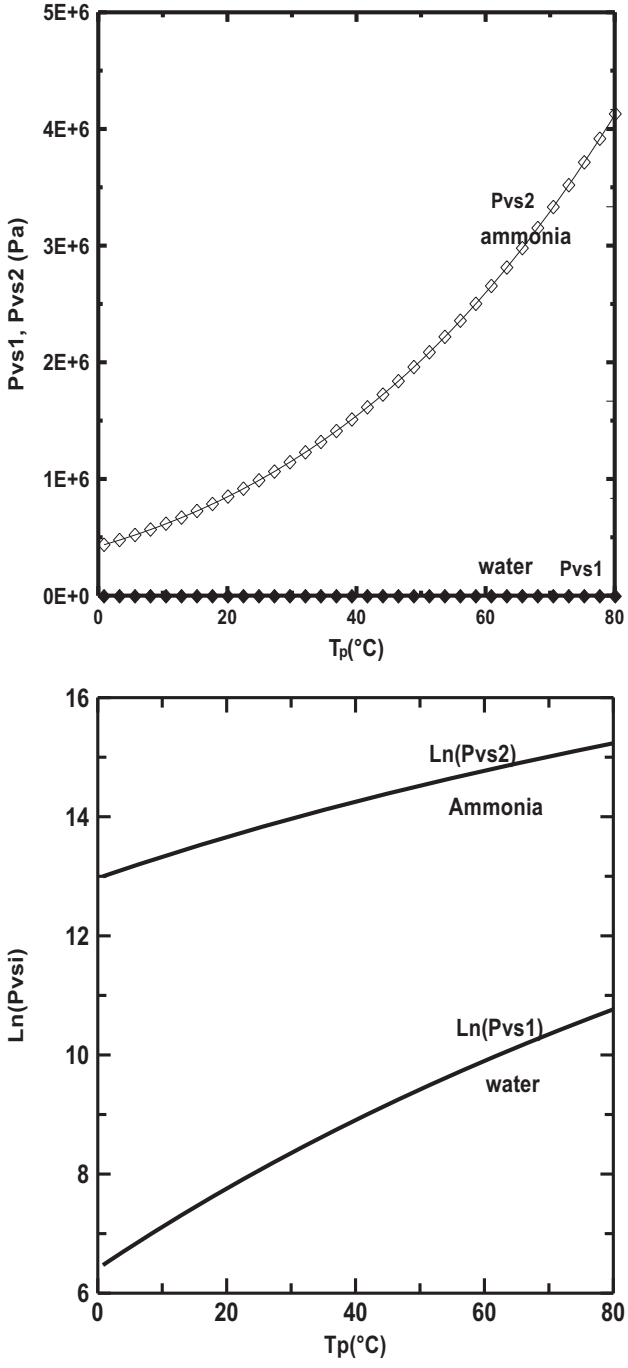

Fig. 2. The saturated pressure profiles of water and of ammonia with the wall temperature.

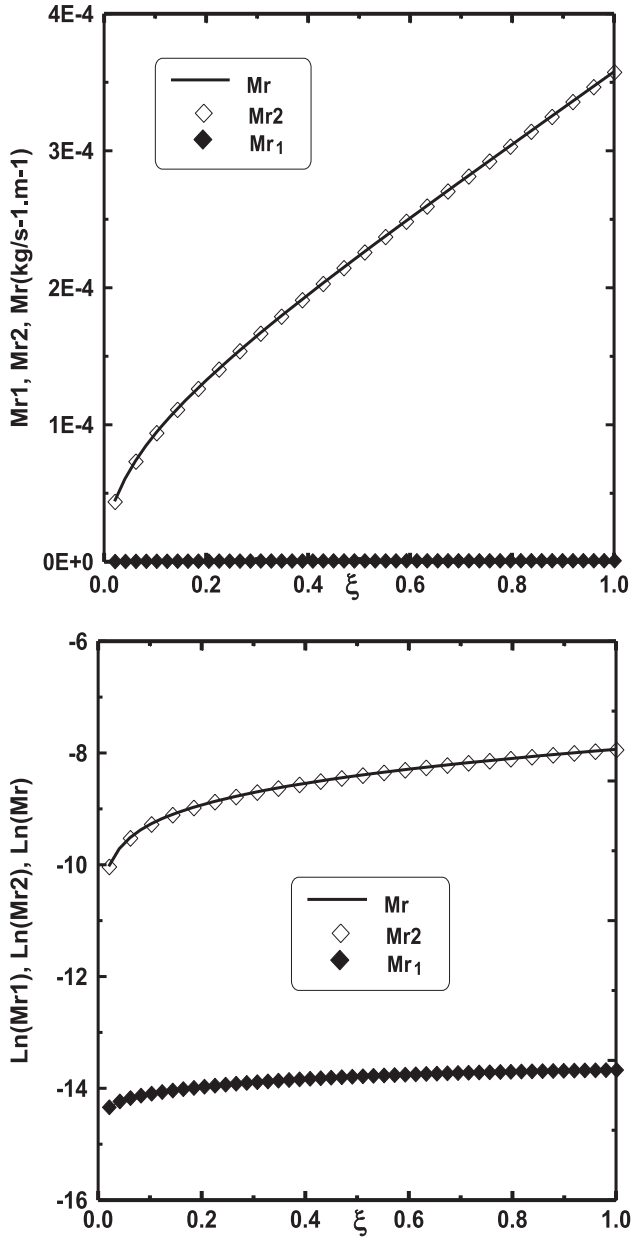

Fig. 3. Axial distribution of the cumulated evaporation rate of water (Mr1), of ammonia (Mr2) and of liquid mixture (Mr = Mr1 + Mr2): $T_{0L} = 10$ ℃, $T_0 = 20$ ℃, $q_1 = 0$, $m_{0L} = 0.001$ kg/m s, $c_{Liq,ammonia} = 0.5$ (50% water–ammonia mixture).

$$\frac{1}{\delta}\mu_L\frac{\partial u_L}{\partial \eta_L}\Big)_{\eta_L=1} = \frac{1}{d-\delta}\mu\frac{\partial u}{\partial \eta}\Big)_{\eta=0};\ \dot{m}_i = \dot{m}c_{Li} - \frac{\rho_l D_l}{\delta}\frac{\partial c_{Li}}{\partial \eta_l}\Big)_{\eta_l=1} = \dot{m}c_i - \frac{\rho D_{g,im}}{d-\delta}\frac{\partial c_i}{\partial \eta}\Big)_{\eta=0} \quad (19)$$

In order to evaluate the importance of the different processes of energy transfer, the following quantities are used [8–11]:

The cumulated evaporation rate of species i at the interface is given by:

$$\mathrm{Mr}_i(\xi) = \int_0^{\xi} \dot{m}_i(\xi)\, d\xi \quad \text{where } \dot{m}_i(\xi) = \dot{m}c_1 - \frac{\rho D_{g,im}}{d-\delta}\frac{\partial c_i}{\partial y}\Big)_{\eta=0} \tag{20}$$

The cumulated evaporation rate of liquid mixture at the interface is given by:

$$\mathrm{Mr} = \int_0^{\xi} \dot{m}(\xi)\, d\xi = \mathrm{Mr}_1 + \mathrm{Mr}_2 \tag{21}$$

3. Solution method

The present conjugated problem defined by the system of Eqs. (1)–(10) with the boundary and interfacial conditions ((11)–(19)) is solved numerically using a finite difference marching procedure in the downstream direction using rectangular grids in the liquid and gas regions. The mesh is characterized by a longitudinal step $\Delta\xi = 1/(N_\xi - 1)$ and a transversal step $\Delta\eta_L = \frac{1}{N_{\eta_L}-1}$ in liquid and $\Delta\eta = \frac{1}{N_\eta - 1}$ in gas. A fully implicit scheme where the axial convection terms were approximated by the upstream difference and the transverse convection and diffusion terms by the central difference is employed. The discrete equations are resolved line by line from the inlet to the outlet of the channel since flows under consideration are a boundary layer type. To ensure that results were grid independent, the solution was obtained for different grid sizes for a typical case programme test. Table 1 shows that the differences in the total evaporating rate obtained using 51 × (51 + 31) and 151 × (51 + 51) grids are always less than 1%.

4. Results and discussions

The results of this study have been obtained for $d/H = 0.015$; $c_{01} = 0$; $c_{02} = 0$; $u_0 = 0.75$ m/s and $P_0 = 9$ bars.

Fig. 2 shows that the saturated pressure of water is less important than the ammonia and consequently ammonia is more volatile than water. The observation of the curves of Fig. 2 shows that the difference between the saturated pressures of ammonia and of water is important for the higher wall temperature. Fig. 3 shows that the water evaporation rate is clearly negligible compared to that of ammonia (the more volatile component) and consequently the mixture cumulated evaporation rate approaches the ammonia cumulated evaporation rate. This result has been justified by the fact that the saturated pressure of water is clearly negligible compared to that of ammonia and particularly for high temperature values.

One can see that the temperature at the interface liquid–gas increases with an increase in the inlet gas temperature T_0 (Fig. 4) and consequently the

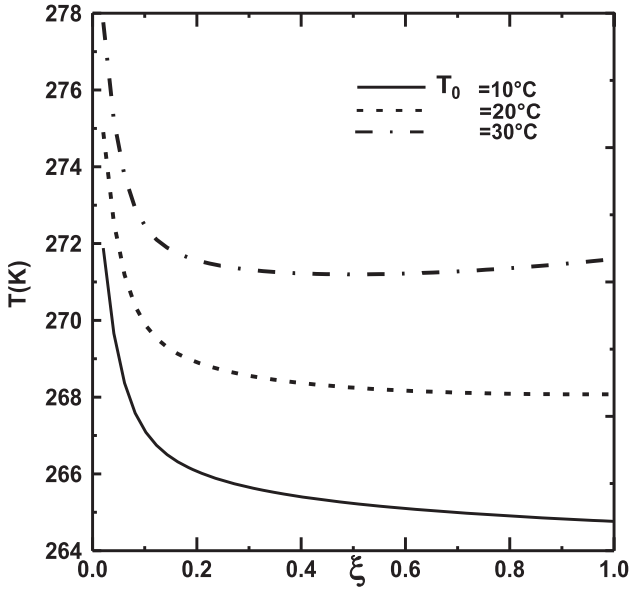

Fig. 4. Influence of inlet gas temperature T_0 on the interfacial temperature: $T_{0L} = 10$°C, $q_1 = 0$, $m_{0L} = 0.001$ kg/m s, $c_{\mathrm{Liq,ammonia}} = 0.5$.

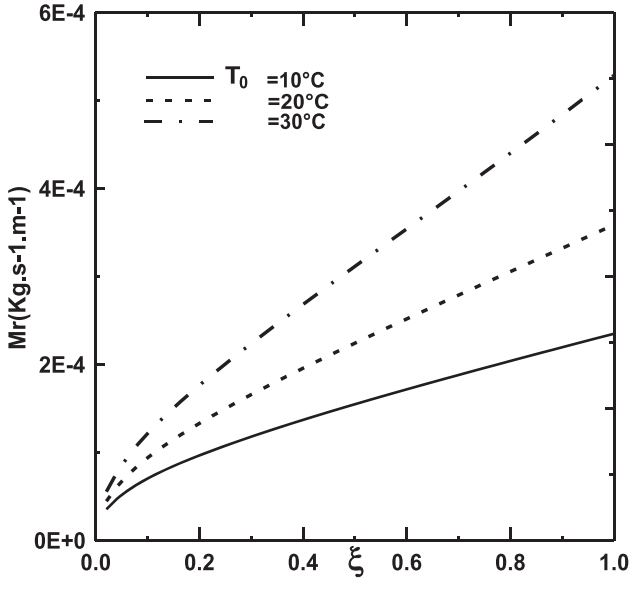

Fig. 5. Effect of the inlet gas temperature T_0 on the cumulated total evaporation rate of liquid mixture Mr: $T_{0L} = 10$°C, $q_1 = 0$, $m_{0L} = 0.001$ kg/m s, $c_{\mathrm{Liq,ammonia}} = 0.5$.

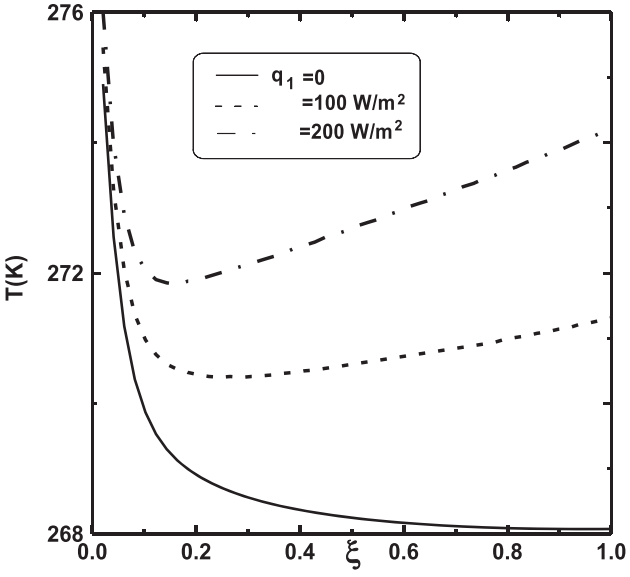

Fig. 6. Effect of the density heat flux q_1 on the interfacial temperature: T_{0L} = 10˚C, T_0 = 20˚C, m_{0L} = 0.001 kg/m s, $c_{Liq,ammonia}$ = 0.5.

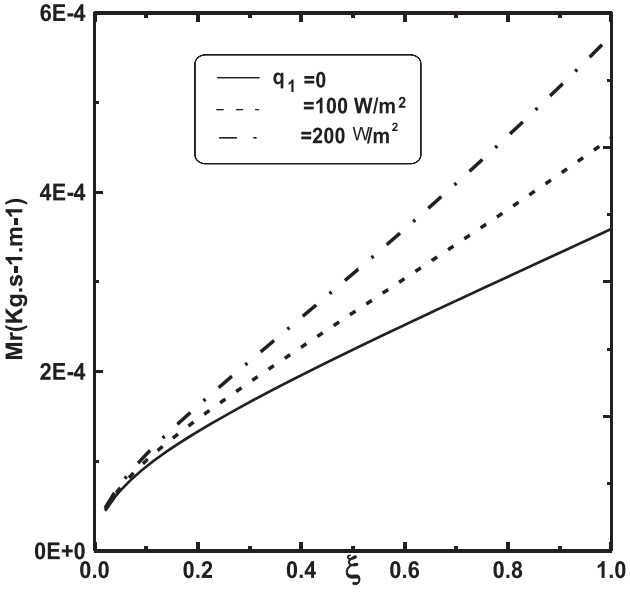

Fig. 7. Effect of the density heat flux q_1 on the cumulated total evaporation rate of liquid mixture Mr: T_{0L} = 10˚C, T_0 = 20˚C, m_{0L} = 0.001 kg/m s, $c_{Liq,ammonia}$ = 0.5.

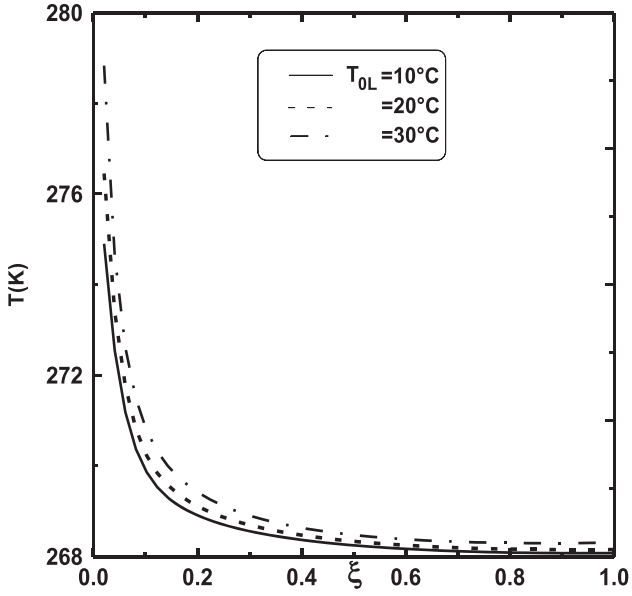

Fig. 8. Effect of the inlet liquid temperature T_{0L} on the interfacial temperature: T_0 = 20˚C, q_1 = 0, m_{0L} = 0.001 kg/m s, $c_{Liq,ammonia}$ = 0.5.

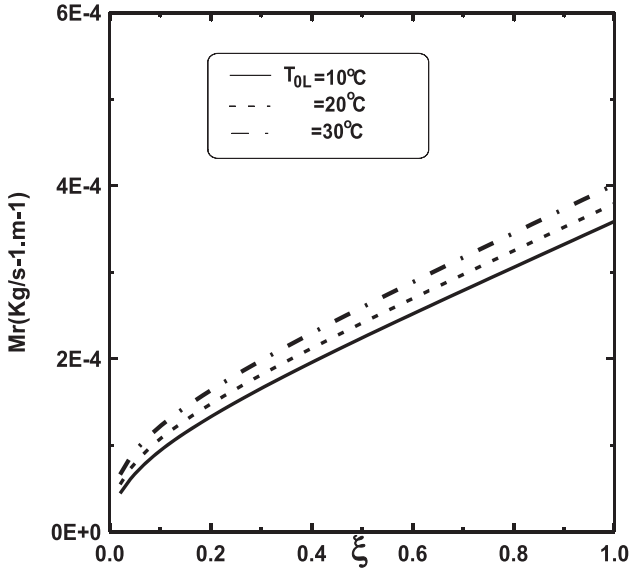

Fig. 9. Effect of the inlet liquid temperature T_{0L} on the cumulated total evaporation rate of liquid mixture Mr: T_0 = 20˚C, q_1 = 0, m_{0L} = 0.001 kg/m s, $c_{Liq,ammonia}$ = 0.5.

evaporation rate of mixture increases (Fig. 5). Fig. 6 reveals that a significant increase in the interfacial temperature when the density heat flux q_1 increases. Consequently, the cumulated evaporation rate of liquid mixture is significantly enhanced when q_1 becomes important (Fig. 7). Fig. 8 illustrates the effect of the inlet liquid temperature T_{0L} on the interfacial temperature. It is shown that an increase in the inlet liquid temperature induces an increase in the interfacial temperature. Consequently, the evaporation rate of the liquid mixture increases (Fig. 9).

Fig. 10 gives the interfacial temperature progression for various inlet liquid mass flow m_{0L}. As expected, the interfacial temperature is higher for a

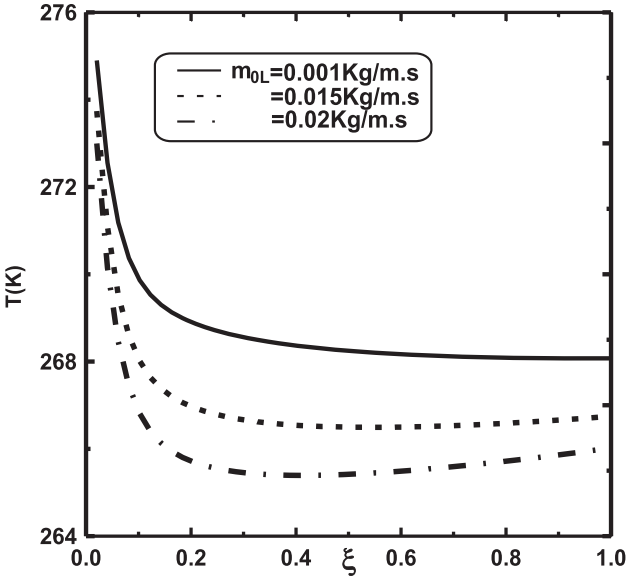

Fig. 10. Influence of the inlet mass flow m_{0L} on the interfacial temperature: $T_{0L} = 10$°C, $T_0 = 20$°C, $q_1 = 0$, $c_{Liq,ammonia} = 0.5$.

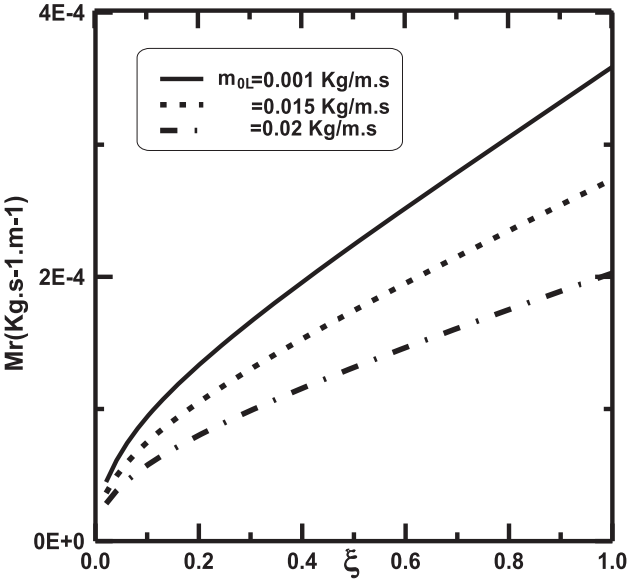

Fig. 11. Effect of inlet mass flow m_{0L} on the cumulated total evaporation rate of liquid mixture Mr: $T_{0L} = 10$°C, $T_0 = 20$°C, $q_1 = 0$, $c_{Liq,amonnia} = 0.5$.

smaller liquid mass flow. Concerning Fig. 11, one can observe that an increase in the inlet liquid mass flow rate inhibits the liquid mixture evaporation. This result can be justified by the fact that, an increase in the inlet liquid mass flow enhances the cooling at the interface liquid–gas and consequently reduces the liquid mixture evaporation. It is found from Fig. 12 that

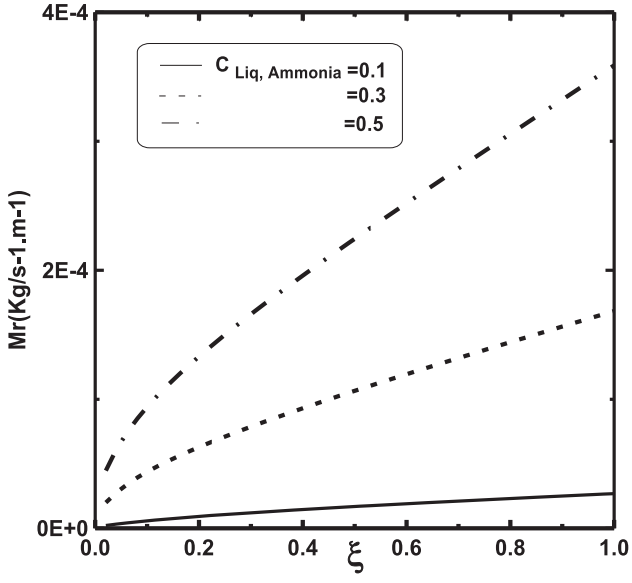

Fig. 12. Influence of inlet liquid concentration of ammonia $c_{Liq,ammonia}$ on the cumulated total evaporation rate of liquid mixture Mr .: $T_{0L} = 10$°C, $T_0 = 20$°C, $q_1 = 0$, $m_{0L} = 0.001$ kg/m s.

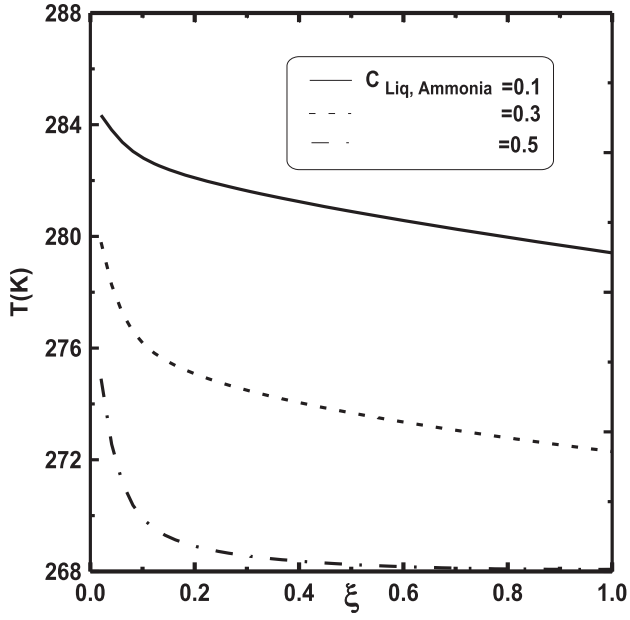

Fig. 13. Influence of the inlet liquid concentration of ammonia $c_{Liq,ammonia}$ on the interfacial temperature liquid–gas: $T_{0L} = 10$°C, $T_0 = 20$°C, $q_1 = 0$, $m_{0L} = 0.001$ kg/m s.

an increase in the inlet liquid concentration of ammonia enhances the liquid mixture evaporation. This result is justified by the fact that the liquid mixture volatility increases with an increase in the inlet liquid concentration of ammonia (the more volatile

component). Therefore, the evaporation rate of liquid mixture increases which results in enhancement of the cooling at the liquid–gas interface. This result is confirmed by that found in Fig. 13.

5. Conclusion

The combined heat and mass transfers during evaporation of a binary liquid film falling on a vertical channel is numerically investigated. The model under investigation is a channel consists of two parallel plates. The first plate is wetted by a mixture liquid film, while the other is dry. The wetted plate is adiabatic and the second plate is isothermal. The influence of the inlet liquid parameters on the coupled heat and mass transfer and on the cumulated evaporation rate of liquid mixture has been studied. The finding of this study can be summarized as follows:

(1) Reducing the amount of liquid film or increasing its inlet temperature benefits the evaporation of binary liquid film.
(2) The combined mass and heat transfer during binary liquid film evaporation strongly affected by the inlet liquid film composition.
(3) The increase in the inlet liquid concentration of ammonia benefits the liquid mixture evaporation and consequently enhances the cooling of the interfacial liquid–gas.

Nomenclature

c_i — mass fraction for species i vapour
c_{0i} — mass fraction for species i vapour in the inlet condition
c_{Li} — mass fraction for species i in the liquid film ($c_{L1} + c_{L2} = 1$)
$c_{\mathrm{Liq,ammonia}}$ — inlet liquid concentration (composition or mass fraction) of ammonia in the liquid mixture ($c_{\mathrm{Liq,ammonia}} = 1 - c_{\mathrm{Liq,water}}$)
c_p — specific heat at constant pressure (J kg^{-1} K^{-1})
c_{pa} — specific heat for air (J kg^{-1} K^{-1})
c_{pvi} — specific heat for species i vapour (J kg^{-1} K^{-1})
d — channel width (m)
$D_{g,im}$ — mass diffusivity of species i vapour in the gas mixture (m^2 s^{-1})
$D_{g,am}$ — mass diffusivity of dry air in the gas mixture (m^2 s^{-1})
D_L — mass diffusivity of species i in the liquid film mixture (m^2 s^{-1})
H — channel length (m)
I — grid point index number in the flow direction
J — grid point index number in transverse direction
L_v — latent heat of evaporation of mixture (J kg^{-1})
L_{vi} — latent heat of evaporation of species i (J kg^{-1})
$\dot{m}_i$ — local evaporation rate of species i (kg s^{-1} m^{-2})
$\dot{m}$ — local evaporation rate of mixture ($\dot{m} = \dot{m}_1 + \dot{m}_2$) (kg s^{-1} m^{-2})
m_{L0} — inlet liquid flow rate (kg s^{-1} m^{-1})
Ma — molecular weight of air (kg mol^{-1})
M_{ri} — total evaporation rate of species i (kg s^{-1} m^{-1})
M_r — total evaporation rate of liquid mixture (kg s^{-1} m^{-1})
M_r^* — total evaporation rate of mixture given by O'Hare and Spedding [6] ($M_r^* = M_r/0.004$)
p — pressure in the channel (N m^{-2})
p_{vsi} — pressure of saturated vapour of species i (N m^{-2})
p^*_{vsi} — partial pressure of species i at the interface liquid–vapour (N m^{-2})
p_{vsm} — pressure of mixture vapour at the interface liquid–vapour ($p^*_{vs1} + p^*_{vs2}$) (N m^{-2})
p_0 — ambiant pressure (N m^{-2})
c_{0Li} — inlet mass fraction for species i in the liquid film ($c_{0L1} = c_{\mathrm{Liq,water}}$ and $c_{0L2} = c_{\mathrm{Liq,ammonia}}$)
T — absolute temperature (K)
T_s — interface temperature (K)
T_w — dry wall temperature (K)
T_p — wetted wall temperature (K)
q_1 — external heat flux of wetted wall (W m^{-2})
q_2 — external heat flux of dry wall (W m^{-2})
q_{Li} — latent heat flux of species i
q_L — latent heat flux of liquid mixture
q_S — sensible heat flux
g — gravitational acceleration (m s^{-2})
R_e — Reynolds number ($R_e = u_0 \cdot d/v_0$)
u — axial velocity (m s^{-1})
v — transverse velocity (m s^{-1})
x — coordinate in the axial direction (m)
x^* — dimensionless axial coordinate
y — coordinate in the transverse direction (m)
w_{Li} — molar fraction of species i in the liquid mixture
w_i — molar fraction of species i vapour

Greek symbols

λ — thermal conductivity of the fluid (W m^{-1} K^{-1})
μ — dynamic viscosity of the fluid (kg m^{-1} s^{-1})

v	—	kinematic viscosity of the fluid ($m^2\ s^{-1}$)
ρ	—	density of the gas ($kg\ m^{-3}$)
η	—	dimensionless coordinate in the transverse direction
ξ	—	dimensionless coordinate in the flow direction
δ	—	liquid film thickness (m)
β	—	thermal expansion coefficient—$1/\rho(\partial\rho/\partial T)_{p,c}$ (K^{-1})
β^*	—	mass expansion coefficient—$1/\rho(\partial\rho/\partial c)_{p,T}$

Subscripts

i	—	species i (1 for water vapour, 2 for ammonia vapour and 3 for dry air)
0	—	inlet condition
L	—	liquid phase
$0L$	—	inlet condition in the liquid phase
a	—	dry air
m	—	mixture
s	—	interface
am	—	dry air in the mixture
im	—	species i in the mixture
Li	—	species i in the liquid

References

[1] B.C. Hoke Jr., J.C. Chen, Mass transfer in evaporating falling liquid film mixtures, AIChE J. 38 (1992) 781–787.

[2] Q. Wang, Mass Transfer Effects in Falling Film Evaporation of Ternary Mixtures. Ph.D. Thesis, Department of Chemical Engineering, Lehigh University, Bethlehem, PA, 1990.

[3] M. Armouzi, X. Chesneau, B. Zeghmati, Numerical study of evaporation by mixed convection of a binary liquid film flowing down the wall of two coaxial cylinders, Heat Mass Transfer 41 (2005) 375–386.

[4] J.W. Palen, Q. Wang, J.C. Chen, Falling film evaporation of binary mixtures, AIChE J. 40 (1994) 207–214.

[5] W.W. Baumann, F. Thiele, Heat and mass transfer in evaporating two-component liquid film flow, Int. J. Heat Mass Transfer 33 (1990) 267–273.

[6] K.D. O'Hare, P.L. Spedding, Evaporation of a binary liquid mixture, Chem. Eng. J. 48 (1992) 1–9.

[7] Z. Ziobrowski, A. Rotkegel, R. Krupiczka, Evaporation of a binary liquid film in the presence of stagnant inert gas, Chem. Process Eng. J. 30 (2009) 13–24.

[8] A.A. Cherif, A. Daïf, Etude numérique du transfert dechaleur et de masse entre deux plaques planes verticalesen présence dun film de liquide binaireruisselant sur lune des plaques chauffée (Numerical study of heat and mass transfer in mixed convection inside a vertical channel with a binary liquid film streaming in one of its heated walls), Int. J. Heat Mass Transfer42 (1999) 2399–2418.

[9] A. Agunaoun, A. Il Idrissi, A. Daif, R. Barriol, Etude de l'évaporation en convection mixte d'un film liquide d'un mélange binaire s'écoulant sur un plan incliné soumis à un flux de chaleur constant (Study of the evaporation in mixed convection of a liquid film of a binary mixture flowing on an inclined plane subjected to a constant heat flux), Int. J. Heat Mass Transfer 41 (1998) 2197–2210.

[10] A. Nasr, C. Debbissi Hfaiedh, S. Ben Nasrallah, Numerical study of evaporation by mixed convection of a binary liquid film, Energy 36 (2011) 2316–2327.

[11] C.D. Hfaiedh, A. Nasr, S. Ben Nasrallah, Evaporation of a binary liquid film flowing down the wall of two vertical plates, Int. J. Therm. Sci. 72 (2013) 34–46.

[12] R.C. Reid, T.K. Sherwood, The Properties of Gases and Liquids, McGraw-Hill, New York, NY, 1958.

[13] R.B. Bird, W.E. Stewart, E.N. Lightfoot, Transport Phenomena, Wiley, New York, NY, 1960.

[14] M. El Armouzi, Étude numérique de l'évaporation en convection mixte d'un film liquide binaire ruisselant sur l'une des parois de deux cylindres coaxiaux (Numerical study of evaporation by mixed convection of a binary liquid film flowing down the wall of two coaxial cylinders), Thèse de l'Université´ de Perpignan, 2000.

[15] K. Benachour, Contribution à l'étude théorique et expérimentale de l'évaporation en convection mixte d'un film binaire ruisselant sur la paroi interne d'un cylindre vertical (Contribution to the theoretical and experimental study of the evaporation by mixed convection of a binary liquid film flowing down the inner wall of a vertical cylinder), Thèse de l'Université de Perpignan, 2000.

Appendix 1

The summary of derivation of equations

(1) For the liquid phase

Continuity equation

$$\frac{\partial \rho_L u_L}{\partial x} + \frac{\partial \rho_L v_L}{\partial y} = 0$$

x-*momentum equation*

$$\rho_L\left(u_L\frac{\partial u_L}{\partial x} + v_L\frac{\partial u_L}{\partial y}\right) = -\rho_L g - \frac{\mathrm{d}P}{\mathrm{d}x} + \frac{\partial}{\partial}\left(\mu_L\frac{\partial u_L}{\partial y}\right)$$

Energy equation

$$\rho_L c_{pL}\left(u_L\frac{\partial T_L}{\partial x} + v_L\frac{\partial T_L}{\partial y}\right) = \frac{\partial}{\partial y}\left(\lambda_L\frac{\partial T_L}{\partial y}\right) + \rho_L D_L(c_{pL,1} - c_{pL,2})\frac{\partial T_L}{\partial y}\frac{\partial c_{L1}}{\partial y}$$

Species diffusion equations

$$u_L\frac{\partial c_{Li}}{\partial x}+v_L\frac{\partial c_{Li}}{\partial y}=\frac{1}{\rho_L}\frac{\partial}{\partial y}\left(\rho_L D_L\frac{\partial c_{Li}}{\partial y}\right);\quad i=1,\ 2$$

The overall mass balance

$$\int_0^{\delta}\rho_L u_L\,dy=m_{0L}+\int_0^{x}\rho v(x,\,0)\,dx$$

(2) For the gaseous phase

Continuity equation

$$\frac{\partial\rho u}{\partial x}+\frac{\partial\rho v}{\partial y}=0$$

x-*momentum equation*

$$u\frac{\partial u}{\partial x}+v\frac{\partial u}{\partial y}=-\frac{1}{\rho}\frac{dP}{dx}-\beta g(T-T_0)-g\sum_{i=1}^{2}\beta_i^*(c_i-c_{i0})+\frac{1}{\rho}\frac{\partial}{\partial}\left(\mu\frac{\partial u}{\partial y}\right)$$

Energy equation

$$\rho c_p\left(u\frac{\partial T}{\partial x}+v\frac{\partial T}{\partial y}\right)=\frac{\partial}{\partial y}\left(\lambda\frac{\partial T}{\partial y}\right)+\rho\sum_{i=1}^{2}\left(D_{g,im}c_{pi}-D_{g,am}c_{pa}\right)\frac{\partial T}{\partial y}\frac{\partial c_i}{\partial y}$$

Species diffusion equations

$$u\frac{\partial c_i}{\partial x}+v\frac{\partial c_i}{\partial y}=\frac{1}{\rho}\frac{\partial}{\partial y}\left(\rho D_{g,im}\frac{\partial c_i}{\partial y}\right);\quad i=1,\ 2,\ 3$$

where $c_1 + c_2 + c_3 = 1$.

The overall mass balance described by the following equation should be satisfied at every axial location:

$$\int_{\delta}^{d}\rho u\,dy=(d-\delta)\rho_0 u_0+\int_0^{x}\rho v(x,\,0)\,dx$$

(3) Equations transformation

In order to fix the position of the liquid–gas interface, we introduce the following transformations (Fig. 1(b)):

In the gaseous phase:

$$\eta=(y-\delta)/(d-\delta),\ \xi=x/H$$

In the liquid phase:

$$\eta_L=y/\delta,\ \xi=x/H$$

$$\xi=x/H \text{ et } \eta_L=y/\delta(\mathrm{x})$$

(4) In the liquid phase

$$\frac{\partial}{\partial y}=\frac{1}{\delta(x)}\frac{\partial}{\partial\eta_L}\text{ et }\frac{\partial}{\partial x}=\frac{1}{H}\frac{\partial}{\partial\xi}-\frac{\eta_1}{\delta(x)H}\frac{\partial\delta}{\partial\xi}\frac{\partial}{\partial\eta_L}$$

Adopting these transformations, the equations governing the flow and heat and mass transfers in the liquid phase are as follows.

Continuity equation

$$\frac{\partial\rho_L u_L}{\partial\xi}-\frac{\eta_L}{\delta}\frac{\partial\delta}{\partial\xi}\frac{\partial\rho_L u_L}{\partial\eta_L}+\frac{H}{\delta}\frac{\partial\rho_L v_L}{\partial\eta_L}=0$$

x-*momentum equation*

$$u_L\frac{\partial u_L}{\partial\xi}+\left(v_L\frac{H}{\delta}-u_L\frac{\eta_L}{\delta}\frac{\partial\delta}{\partial\xi}\right)\frac{\partial u_L}{\partial\eta_L}=-\frac{1}{\rho_L}\frac{\mathrm{d}P}{\mathrm{d}\xi}-\frac{H}{\rho_L\delta^2}\frac{\partial}{\partial\eta_L}\left[\mu_L\frac{\partial u_L}{\partial\eta_L}\right]+gH$$

Energy equation

$$u_L\frac{\partial T_L}{\partial\xi}+\left(u_L\frac{\eta_L-1}{\delta}\frac{\partial\delta}{\partial\xi}+\frac{H}{\delta}v_L\right)\frac{\partial T_L}{\partial\eta_L}=\frac{1}{\rho_L c_{pL}}\left\{\frac{H}{\delta^2}\frac{\partial}{\partial\eta_L}\left(\lambda_L\frac{\partial T_L}{\partial\eta_L}\right)+\rho_L D_L\left(c_{pL,1}-c_{pL,2}\right)\frac{H}{\delta^2}\frac{\partial T_L}{\partial\eta_L}\frac{\partial c_{L,1}}{\partial\eta_L}\right\}$$

Species diffusion equations

$$u_L\frac{\partial c_{Li}}{\partial\xi}+\left(u_L\frac{\eta_L-1}{\delta}\frac{\partial\delta}{\partial\xi}+\frac{H}{\delta}v_L\right)\frac{\partial c_{Li}}{\partial\eta_L}=\frac{1}{\rho_L}\frac{H}{\delta^2}\frac{\partial}{\partial\eta_L}\left(\rho_L D_{Li}\frac{\partial c_{Li}}{\partial\eta_L}\right);\quad i=1,\ 2$$

The overall mass balance

$$\int_0^{1}\delta\rho_L u_L\,d\eta_L=\left[m_{0L}-H\int_0^{\xi}\rho v(\xi,\ \eta=0)\,d\xi\right]$$

(5) In the gas phase

$$\frac{\partial}{\partial y}=\frac{1}{d-\delta(x)}\frac{\partial}{\partial \eta} \text{ et } \frac{\partial}{\partial x}=\frac{1}{H}\frac{\partial}{\partial \xi}+\frac{\eta-1}{(d-\delta(x))}\frac{1}{H}\frac{\partial \delta}{\partial \xi}\frac{\partial}{\partial \eta}$$

Adopting these transformations, the equations governing the flow and heat and mass transfers in the in the gas phase are as follows.

Continuity equation

$$\frac{\partial \rho u}{\partial \xi}+\frac{\eta-1}{d-\delta}\frac{\partial \delta}{\partial \xi}\frac{\partial \rho u}{\partial \eta}+\frac{H}{d-\delta}\frac{\partial \rho v}{\partial \eta}=0$$

x-*momentum equation*

$$u\frac{\partial u}{\partial \xi}+\left(\frac{\eta-1}{d-\delta}\frac{\partial \delta}{\partial \xi}u+\frac{H}{d-\delta}v\right)\frac{\partial u}{\partial \eta}=-\frac{1}{\rho}\frac{\mathrm{d}P}{\mathrm{d}\xi}-g\beta H(T-T_0)-gH\sum_{i=1}^{2}\beta_i^*(c_i-c_{0i})+\frac{1}{\rho}\frac{H}{(d-\delta)^2}\frac{\partial}{\partial \eta}\left(\mu\frac{\partial u}{\partial \eta}\right)$$

Energy equation

$$u\frac{\partial T}{\xi}+\left(u\frac{\eta-1}{d-\delta}\frac{\partial \delta}{\partial \xi}+\frac{H}{d-\delta}v\right)\frac{\partial T}{\partial \eta}=\frac{1}{\rho C_\rho}\left\{\frac{H}{(d-\delta)^2}\frac{\partial}{\partial \eta}\left(\lambda\frac{\partial T}{\partial \eta}\right)+\rho\sum_{i=1}^{2}(D_{g,im}c_{pi}-D_{g,am}c_{pa})\frac{H}{(d-\delta)^2}\frac{\partial T}{\partial \eta}\frac{\partial c_i}{\partial \eta}\right\}$$

Species diffusion equations

$$u\frac{\partial c_i}{\partial \xi}+\left(u\frac{\eta-1}{d-\delta}\frac{\partial \delta}{\partial \xi}+\frac{H}{d-\delta}v\right)\frac{\partial c_i}{\partial \eta}=\frac{1}{\rho}\frac{H}{(d-\delta)^2}\frac{\partial}{\partial \eta}\left(\rho D_{g,im}\frac{\partial c_i}{\partial \eta}\right);\quad i=1,\ 2$$

The overall mass balance

$$\int_0^1 \rho(d-\delta)u(\xi,\ \eta)\,d\eta=\left[(d-\delta_0)\rho_0 u_0+H\int_0^\xi \rho v(\xi,\ \eta=0)\,d\xi\right]$$